Segmentation of 3D CT Volume Images Using a Single 2D Atlas *

Feng Ding[1], Wee Kheng Leow[1], and Shih-Chang Wang[2]

[1] Dept. of Computer Science, National University of Singapore,
3 Science Drive 2, Singapore 117543
dingfeng, leowwk@comp.nus.edu.sg
[2] Dept. of Diagnostic Radiology, National University of Singapore,
5 Lower Kent Ridge Road, Singapore 119074
dnrwsc@nus.edu.sg

Abstract. Segmentation of medical images is an important first step in the analysis of medical images. A lot of research has been performed on the segmentation of complex CT/MR images using the atlas-based approach. Most existing methods use 3D atlases which are more complex and difficult to control than 2D atlases. They have been applied mostly for the segmentation of brain images. This paper presents a method that can segment multiple slices of an abdominal CT volume using a single 2D atlas. Segmentation of human body images is considerably more difficult and challenging than brain image segmentation. Test results show that our method can handle large variations in shape and intensity between the atlas and the target CT images.

1 Introduction

Segmentation of medical images is an important first step in the analysis of medical images. For example, in liver transplant, CT images of the donor are taken. Then, the image regions corresponding to the liver are segmented to compute the liver's volume. Moreover, 3D model of the liver and the blood vessels are reconstructed to help the surgeons plan the surgical procedure.

A lot of research has been performed on the segmentation of CT and MR images. In particular, the atlas-based approach is most suited to segmenting complex medical images because it can make use of spatial and structured knowledge in the segmentation process. Typically, 3D atlases are used to segment the surfaces of the anatomical structures in 3D CT/MR images [1–7]. However, 3D atlases are more complex and difficult to construct than 2D atlases. There are much more parameters to control in 3D atlases. Thus, 3D atlas-based algorithms tend to be developed for segmenting specific anatomical structures. It is not easy to adapt the algorithms to the segmentation of other anatomical structures by simply changing the atlas.

An alternative is to use multiple 2D atlases to segment a CT/MR volume. In this case, it is necessary to understand how many 2D atlases will be needed to

* This research is supported by NUS ARF R-252-000-210-112.

segment all the slices in a volume. The worst case scenario of one atlas per image would defeat the idea of using 2D atlases because the stack of 2D atlases would contain the same amount of complexity as a 3D atlas. It also makes practical application difficult because there are many slices in a typical CT/MR volume. For example, in the case of liver transplant, more than 200 abdominal CT images are taken.

Interestingly, most work on atlas-based segmentation has been focused on brain MR images [1–3, 8, 6] or heart MR images [4, 7]. Less work is done on the segmentation of abdominal CT images [5], which is considerably more difficult and challenging than segmentation of brain images.

This paper describes an atlas-based method for segmenting multiple anatomical structures in multiple slices of an abdominal CT volume using a single 2D atlas. The research objective is to investigate how well can a single 2D atlas perform on segmenting various slices in a CT volume of a particular patient. This research can lead to an understanding of the number and types of atlas required to segment various CT images encountered in normal clinical practices.

Test results show that our algorithm can successfully and accurately segment 34 abdominal CT slices of 1mm thickness using a single 2D atlas. Since the 2D atlas differs significantly in shape and intensity from the test CT images, successful test results suggest that the algorithm should work well in segmenting CT images of other patients. Our research work thus contributes to solving the difficult and challenging problem of segmenting human body CT/MR images.

2 Related Work

Atlas-based segmentation is performed using atlas-based registration technique. The registered atlas contours (2D case) and surfaces (3D case) are taken as the boundaries of the segmented anatomical structures. Fully automatic atlas-based segmentation problems map to atlas-based registration problems with unknown correspondence. Solutions to these problems have to solve both the registration and the correspondence problems at the same time. These problems are therefore much more difficult to solve than semi-automatic registration and segmentation, which require some user inputs such as landmark points [9].

An atlas-based segmentation algorithm typically comprises two complementary stages: (1) global transformation of the atlas to roughly align it to the target image, and (2) local transformation or deformation of the atlas to accurately register it to the corresponding image features. Global transformation often serves to provide a good initialization for local deformation. Without a good initialization, local deformation may deform the atlas out of control and extract wrong object boundaries (see Section 3.3 for an example).

In the global transformation stage, spatial information (i.e., relative positions) of various parts of an atlas is used to determine how the atlas should be transformed. Both similarity [2, 3, 5] and affine [4, 6, 7] transformations have been used. An iterative optimization algorithm is applied to compute the optimal transformation parameters. In each iteration, the possible correspondence

between the atlas and the target is usually determined based on the closest point criterion in the same way as the Iterative Closest Point algorithm [10].

In the local deformation stage, several main approaches have been adopted. The method in [11] applies iterative optimization to determine optimal local affine or 2nd-order polynomial transformations that deform the various parts of the atlas to best match the target. The methods in [4, 5] also apply optimization techniques but they represent the 3D atlas surface using B-splines and thin-plate spline constraint. These methods ensure that the extracted surfaces are smooth but they require a large number of parameters to represent complex convoluted surfaces of the brain.

A popular method is to apply the so-called *demons algorithm* [2, 3, 6, 12]. It regards the atlas and the target as images at consecutive time steps, and applies the optical flow algorithm to determine the correspondence between them. As for any optical flow algorithm, it suffers from the so-called *aperture problem* and may not be able to handle large displacements between corresponding points. It is also easily affected by noise and extraneous image features.

Among the existing methods discussed in this section, [5, 7] use probabilistic atlases whereas the other methods use non-probabilistic atlases. Although probabilistic atlas contains more information about the variations, it requires sufficient training samples to accurately model the probability distributions.

In addition to applying atlas-based registration technique, [5, 7] included a final classification stage that classifies each pixel to a most likely anatomical category. This stage is required because the registration algorithms are not precise enough in aligning the atlas boundaries to the object boundaries in target images. Classification approach can improve the accuracy of the segmentation result. However, it may not be able to handle segmentation of regions which are nonuniform in intensity and texture. For example, the air pocket in the stomach appears to have the same intensity as the background (Section 4, Fig. 3a, 5). Classification algorithms will be easily confused by such nonuniform regions.

Some existing papers have presented quantitative performance measures of their methods. In particular, [2, 3] measure similarity index that is proportional to the area of intersection between segmented regions and the ground truth, [12, 5] measure the amounts of false positives and false negatives, and [6] measures the mean squared error of corresponding points between the extracted boundaries and ground truth.

3 Automatic Atlas-Based Segmentation

Our method uses a 2D deformable atlas to segment the major components in abdominal CT images. The atlas consists of a set of closed contours of the entire human body, liver, stomach, and spleen, which are manually segmented from a reference CT image given in [13]. As shown in Fig. 1, the reference image is significantly different from the target image in terms of shapes and intensities of the body parts. Such differences are common in practical applications.

Our fully automatic segmentation algorithm consists of three stages:

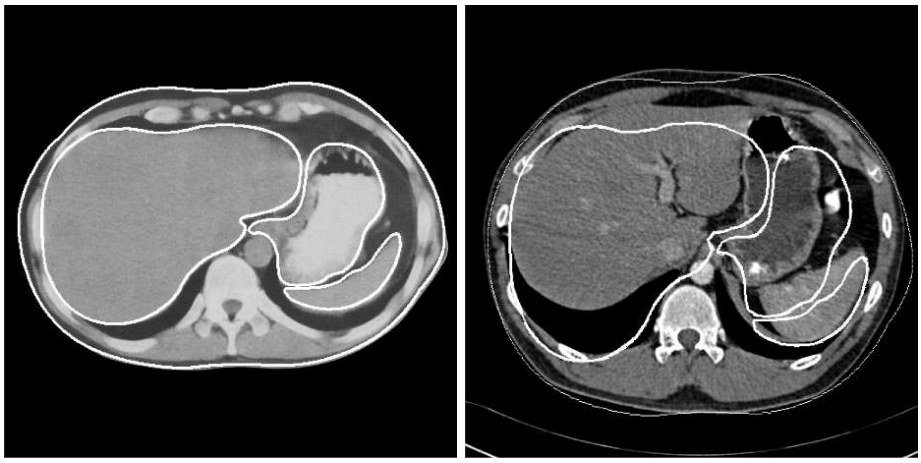

(a) (b)

Fig. 1. (a) Atlas contours (white curves) superimposed on the reference CT image taken from [13]. (b) Atlas registered onto an target image after global transformation.

1. Global transformation of the entire atlas.
2. Iterative local transformation of individual parts in the atlas.
3. Atlas contour refinement using active contour algorithm.

3.1 Global Transformation

This stage performs registration of the atlas to the target input image with *unknown correspondence*. First, the outer body contour of the target image (target contour) is extracted by straightforward contour tracing. Next, the outer body contour of the atlas (reference contour) is registered under affine transformation to the target contour using Iterative Closest Point algorithm [10]. After registration, the correspondence between the reference and target contour points is known. Then, the affine transformation matrix between the reference and target contours is easily computed from the known correspondence by solving a system of over-constrained linear equations. This transformation matrix is then applied to the atlas to map the contours of the inner body parts to the target image.

After global transformation, the centers of the reference contours fall within the corresponding body parts in the target image (Fig. 1b). The reference contours need to be refined to move to the correct boundaries of the body parts.

3.2 Iterative Local Transformation

This stage iteratively applies local transformations to the individual body parts to bring their reference contours closer to the target contours. The idea is to search the local neighborhoods of reference contour points to find possible corresponding target contour points. To achieve this goal, it is necessary to use

features that are invariant to image intensity because the reference and target images can have different intensities (as shown in Fig. 1).

Let $N(p)$ denote the normal to the reference contour at point p, and $L(p)$ denote an ordered list of points $\{p_i\}$, $i = -n, \ldots, 0, \ldots, n$, lying on $N(p)$, with $p_0 = p$. Let $I(p_i)$ denote the intensity of point p_i. Then, the ordered list $D(p) = \{I(p_i) - I(p_{i+1})\}$, $i = -n, \ldots, n-1$, is the *intensity difference distribution* (IDD) at p along $N(p)$. IDD depends only on the local intensity difference, which does not differ as much as intensity across images. Thus, IDD is better than intensity for determining corresponding points between the images. In the same way, we can compute the IDD $D'(p')$ of an image point p' along a normal $N(p)$ of the reference contour and with respect to the target image intensities $I'(p'_i)$. In the current implementation, $n = 5$, i.e., the length of IDD is 10.

The local search for possible corresponding points is performed as follows, after coarse registration of the atlas and the reference image to the target image by global transformation. For each reference contour point p, a search is performed within a small neighborhood $U(p)$ centered at p and along the normal $N(p)$ for a target image point p' whose IDD $D'(p')$ is most similar to $D(p)$. The difference between $D(p)$ and $D'(p')$ is measured in terms of the Euclidean distance between them. The neighborhood $U(p)$ decreases quadratically over time so that the search process will converge. In the current implementation, the width of the search neighborhood is 100 at the first iteration.

After finding the best matching target image point p' of a reference contour point p, a verification procedure is performed. Shoot a ray from the centroid of the closed reference contour of p to p'. If the number of number of "white" pixels or "black" pixels along the ray in the target image exceeds a predefined threshold, then the point p' is discarded because the intensity of the desired body parts are gray. Otherwise, p' is regarded as a corresponding point of p.

Given the reference contour points p_i whose corresponding points p'_i are found, compute the affine transformation matrix M that maps p_i to p'_i. Then, the matrix M is applied to all reference contour points, including those whose corresponding points are not found.

The above local transformation is repeated iteratively for each closed contour of the body parts individually until the reference contours converge. Therefore, the reference contours of different body parts can be mapped to the corresponding target image contours through different affine transformation matrices that are appropriate for them.

The iterative local transformation algorithm described above is analogous to the Iterative Closest Point (ICP) algorithm [10] in that it iteratively determines the possible correspondence between the reference and the target, and computes the transformation that maps the reference to the target. However, it differs from ICP in that possible correspondence is determined based on most similar IDD, which is a local image feature, instead of nearest position as in ICP. Therefore, it can determine the correct correspondence more accurately than ICP. This algorithm can thus be called an *Iterative Corresponding Point* algorithm. Sample results of iterative local transformation are shown in Fig. 2.

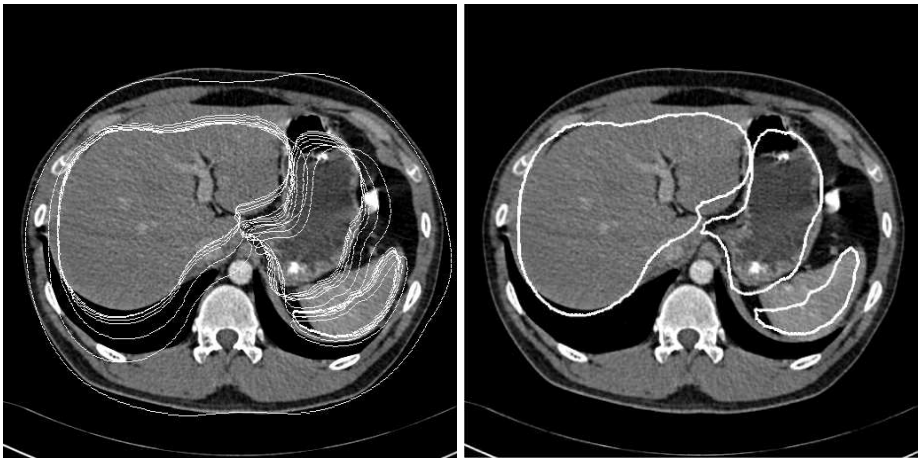

(a) (b)

Fig. 2. Iterative local transformation. (a) The white reference contours are iteratively transformed. (b) The result of iterative local transformation after convergence.

3.3 Atlas Contour Refinement

The last stage performs refinement of the atlas contour using active contour, i.e., snake algorithm [14] with Gradient Vector Flow (GVF) [15]. The original snake algorithm has the shortcoming of not being able to move into concave parts of the objects to be segmented. This is because there is no image forces outside the concave parts to attract the snake. GVF diffuses the gradient vectors of the edges outward, and uses the gradient vectors as the image forces to attract the snake into concave parts.

Figure 3(a) illustrates the result of applying snake with GVF on the atlas to refine the contours obtained from iterative local transformation. The final atlas contours now coincide accurately with the actual boundaries of the body parts in the target image.

Note that after global transformation, the discrepancies between the reference contours and the target contours are still quite large (Fig. 1b). If the snake algorithm is applied immediately after global transformation without iterative local transformation, the reference contour is easily attracted to the boundary edges of other body parts (Fig. 3b). This shows that generic deformable models such as active contour (i.e., snake), active shape, and level set can be easily attracted to incorrect boundary edges. Our method resolves this problem by using iterative local transformation to bring the atlas contours closer to the desired object boundaries before applying the snake algorithm.

3.4 Comparisons with Existing Work

Most existing atlas-based approaches adopt a two-stage approach consisting of global transformation followed by local deformation. On the other hand, our

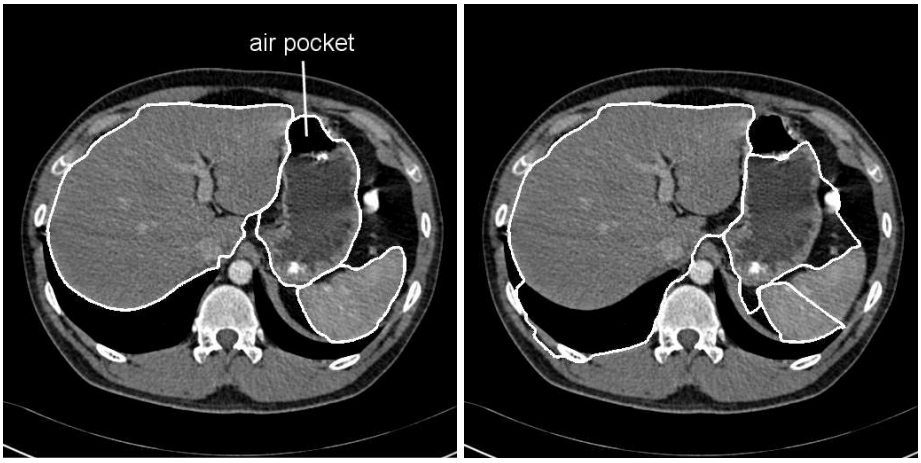

(a) (b)

Fig. 3. Results after contour refinement by snake algorithm. (a) With iterative local transformation (slice 72). (b) Without iterative local transformation.

method consists of three stages, namely (1) global affine transformation, (2) iterative local affine transformation, and (3) snake deformation. The first two stages are similar to those in [1], but the method in [1] is developed for registering an atlas to a brain surface that is already segmented.

[5] also presented a method for segmenting abdominal CT images. However, their atlas registration algorithm is not accurate enough, and a final classification stage is applied to classify the image pixels into various anatomical categories. In contrast, by adopting a three-stage approach, our atlas registration algorithm is accurately enough to segment the various anatomical parts. Compare to the test results reported in [5, 8], our method can handle much more variations between the atlas and the target images.

4 Experiments and Discussion

40 abdominal CT images (from slice 41 to 80) of 1mm thickness of a patient were used in the test. The accuracy of the segmentation result was measured in terms of the area of intersection between the target body part (that was obtained manually) and the segmented regions. This performance measure, called *similarity index* S, was proposed by Zijdenbos et al. [16]:

$$S = 2\frac{|A \cap B|}{|A| + |B|} \tag{1}$$

where A is the set of pixels of the body part in the target image and B that of the segmented region. When the segmented region coincide exactly with the target body part, $S = 1$.

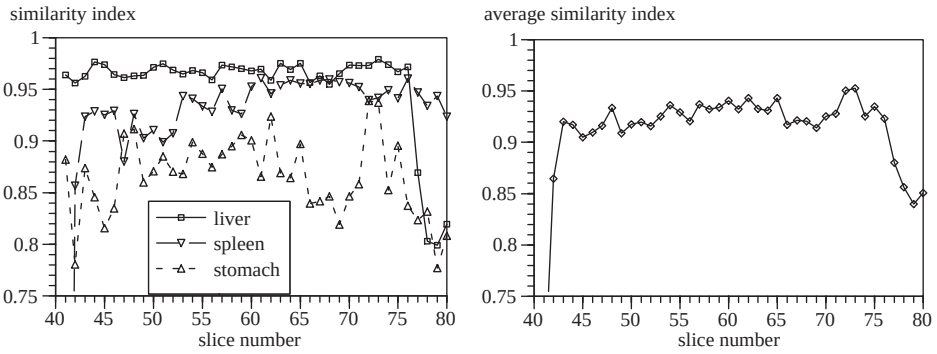

(a) (b)

Fig. 4. Test results. (a) Similarity indices of liver, spleen, and stomach. (b) Average similarity index.

Detailed segmentation performance of the algorithm is shown in Fig. 4. The liver is well segmented and the algorithm's performance on liver is very stable (Fig. 4a). The similarity indices are greater than 0.95 for slices 41 to 76 (Fig. 3a, 5). From slice 77 onward, the liver is split into two lobes, which is greatly different from that in the atlas image (Fig. 6b).

The algorithm's performance on segmenting the spleen shows a bit variation (Fig. 4a). But the similarity indices are still higher than 0.9 for slices 43 to 80 (Fig. 3a, 5). For slice 42, the spleen becomes so small that it differs significantly from that in the atlas (Fig. 6a). Thus, the algorithm is not expected to perform well for this case.

The stomach is less well segmented, with the similarity index ranging from 0.8 to 0.95. It is due to the existence of air pocket, which appears as a black region with a very thin wall (Fig. 3a, 5b). When the air pocket is correctly included in the segmentation result (Fig. 3a), or when there is no air pocket (Fig. 5a), then the similarity index is high. The shape of stomach is quite complex. So, sometimes the snake algorithm is attracted to nearby edges that actually belong to the liver and the spleen.

Figure 4(b) illustrates the average performance of the algorithm on segmenting the liver, spleen, and stomach. The similarity index is above 0.9 for slices 43 to 76 (Fig. 3a, 5). That is, with a single 2D atlas, the algorithm can successfully and accurately segment 34 slices of the abdominal CT volume.

5 Conclusions

This paper presented an atlas-based method for segmenting abdominal CT images. It applies three complementary stages, namely global transformation, iterative local transformation, and snake algorithm, to iteratively deform the atlas to register with the target image. Experimental tests show that the algorithm

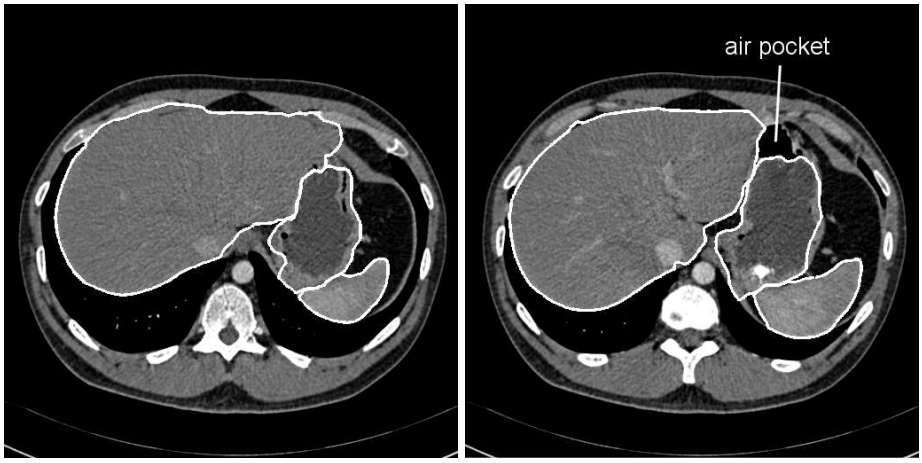

(a) (b)

Fig. 5. Results with high similarity indices. (a) Segmentation results of slice 48. (b) Segmentation results of slice 60.

can successfully and accurately segment 34 slices of a CT volume of 1mm thickness using a single 2D atlas. As the reference image that is used to derive the atlas differs significantly in shape and intensity from the target CT images, the successful test results suggest that the algorithm should work well on segmenting CT images of different patients. This research work thus contributes to solving the difficult and challenging problem of segmenting human body images.

References

1. Thurfjell, L., Bohm, C., Greitz, T., Eriksson, L.: Transformations and algorithms in a computerized brain atlas. IEEE Tran. on Nuclear Science **40** (1993) 1187–1191
2. Dawant, B.M., Hartmann, S.L., Thirion, J.P., Maes, F., Vandermeulen, D., Demaerel, P.: Automatic 3-D segmentation of internal structures of head in MR images using a combination of similarity and free-form transformations: Part I, methodology and validation on normal subjects. IEEE Trans. on Medical Imaging **18** (1999) 909–916
3. Hartmann, S.L., Parks, M.H., Martin, P.R., Dawant, B.M.: Automatic 3-D segmentation of internal structures of head in MR images using a combination of similarity and free-form transformations: Part II, validation on severely atrophied brains. IEEE Trans. on Medical Imaging **18** (1999) 917–926
4. Rueckert, D., Sanchez-Ortiz, G.I., Lorenzo-Valdés, M., Chandrashekara, R., Mohiaddin, R.: Non-rigid registration of cardiac MR: Application to motion modelling and atlas-based segmentation. In: IEEE Int. Symp. on Biomedical Imaging. (2002)
5. Park, H., Bland, P.H., Meyer, C.R.: Construction of an abdominal probabilistic atlas and its application in segmentation. IEEE Trans. on Medical Imaging **22** (2003) 483–492

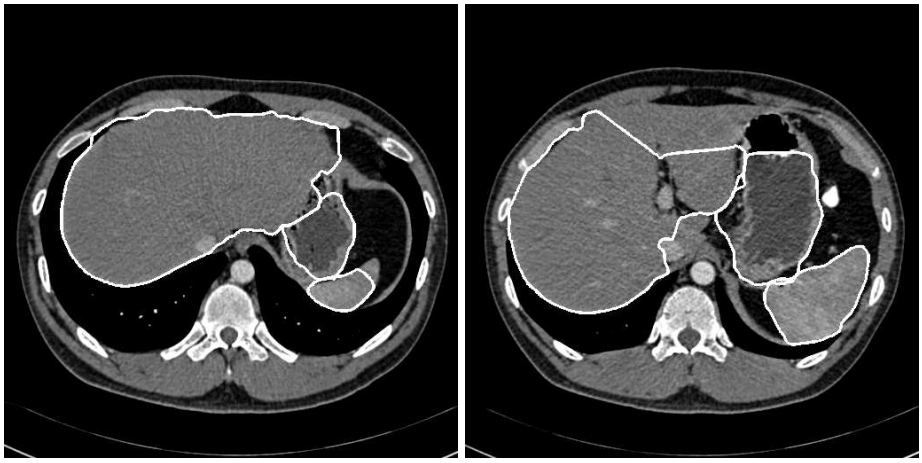

(a) (b)

Fig. 6. Results with relatively low similarity indices. (a) Segmentation results of slice 42. (b) Segmentation results of slice 77.

6. Cuadra, M., Pollo, C., Bardera, A., Cuisenaire, O., Villemure, J.G., Thiran, J.P.: Atlas-based segmentation of pathological MR brain images using a model of lesion growth. IEEE Trans. on Medical Imaging **23** (2004) 1301–1314
7. Lorenzo-Valdés, M., Sanchez-Ortiz, G.I., Elkington, A.G., Mohiaddin, R.H., Rueckert, D.: Segmentation of 4D cardiac MR images using a probabilistic atlas and the EM algorithm. Medical Image Analysis **8** (2004) 255–265
8. Aboutanos, G.B., Nikanne, J., Watkins, N., Dawant, B.M.: Model creation and deformation for the automatic segmentation of the brain in MR images. IEEE Trans. on Biomedical Engineering **46** (1999) 1346–1356
9. Lancaster, J.L., Glass, T.G., R., B., Downs, L.H., Mayberg, H., Fox, P.T.: A modality-independent approach to spatial normalization. Human Brain Mapping **3** (1995) 209–223
10. Besl, P.J., McKay, N.D.: A method for registration of 3-D shapes. IEEE Trans. on Pattern Analysis and Machine Intelligence **14** (1992) 239–256
11. Cuisenaire, O., Thiran, J., Macq, B., Michel, C., Volder, A.D., Marques, F.: Automatic registration of 3D MR images with a computerized brain atlas. SPIE Medical Imaging **1719** (1996) 438–449
12. Aboutanos, G.B., Nikanne, J., Watkins, N., Dawant, B.M.: Model creation and deformation for the automatic segmentation of the brain in MR images. IEEE Trans. on Biomedical Engineering **46** (1999) 1346–1356
13. Fleckenstein, P., Jensen, J.T.: Anatomy in Diagnostic Imaging. Munksgaard (1993)
14. Kass, M., Witkin, A., Terzopoulos, D.: Snakes: active contour models. Int. J. of Computer Vision **1** (1987) 321–331
15. Xu, C., Prince, J.L.: Gradient vector flow: A new external force for snakes. In: Proc. IEEE Conf. on Computer Vision and Pattern Recognition. (1997)
16. Zijdenbos, A.P., Dawant, B.M., Margolin, R.A., Palmer, A.C.: Morphometric analysis of white matter lesions in MR images: Method and validation. IEEE Trans. on Medical Imaging **13** (1994) 716–724